A potential method to detect the orientation of the suspended rod-shaped particles using polarized-light scattering

Ran Liao[1]*
[1]Division of Ocean Science and Technology,
Graduate School at Shenzhen, Tsinghua University,
Shenzhen 518055, China
*liao.ran@sz.tsinghua.edu.cn

Yong Wang[2] and Hui Ma[2]
[2]Institute of optical imaging and sensing,
Graduate School at Shenzhen, Tsinghua University,
Shenzhen 518055, China

***Abstract*—In situ detection of non-spherical particles is very important for the ocean observatory, because they are the majority of the particles in the sea water. However, many of the current commercial instruments assume the spherical particles. In this paper, we present a method which has the potential to detect the orientation of the suspended rod-shaped particles in the fluid field. We use a simultaneous setup to measure the scattered polarization of the fibers suspended in the water and scan along the fluid field. The experimental results indicate that the intensity and degree of polarization (DOP) will change with the field. To explain it, we build a model by combining the fluid field and the scattering of infinitely long cylinders. The simulation based on the model can recover the main aspects of the experimental results. Then, we give the histogram of DOP of the individual fiber, which implies their orientation distribution. Finally, we suggest a method to retrieve the orientation of the fibers by measuring the full Stokes vector.**

***Keywords*— polarized-light scattering, rod-shaped particles,**

I. INTRODUCTION

In situ detection of the particles in the sea is very important for the ocean observatory [1]. Many of the current commercial instruments assume the spherical particles [2]. Unfortunately, the majority of the particles in the sea water are not spherical and even many of them are rod-shaped [3]. When these particles are suspended in the fluid field, their optical scattering of particles are subjected to not only their shape, but also their orientation determined by the interaction with the fluid field.

Polarization has shown the promising application to detect the fibrous tissues [4-6]. And some researches have implied that the scattered polarization is sensitive to shape and the orientation of the suspended non-spherical particles [7-8]. In the early study, we have given the preliminary results about the scattered polarization of the glass fibers in the stirred field [9].

In this paper, we still focus on the influence of the orientation of the suspended rod-shaped particles in the fluid field. We will show the experimental results about the polarized-light scattering of the suspended rod-shaped particles when we scan in the stirred field. And then we will build a new model to explain and qualitatively recover the results. After analysis of the histogram of DOP of the fibers, we will finally suggest a method to detect the orientation of the fibers.

II. SETUP AND METHODS.

The schematic of the experimental setup is shown as Fig.1. In advance, we define the horizontal (H) and vertical (V) polarization states as their directions are parallel and perpendicular to the X-Z plane, respectively.

The sample consists of glass fibers and the water. The fibers' diameters are 10-micron and the lengths are larger than 1mm, and so their aspect ratios exceed 100. The sample is contained in a glass round beaker, and mounted on a platform which can be moved both in X and Z directions by translating stages. And the center area of the stirred fluid field is defined as the origin point, which is assumedly coincide with the center point of the container. The fluid field is generated by a magnetic stirrer which is located on the bottom of the beaker, and the flow suspends the fibers.

An incident polarized light illuminates the sample and is scattered by the fibers to the receiving arm. After that the scattered light is splitted to two orthometric polarization H and V and then detected by two photomultiplier tubes (PMT). The signals are transited to the computer by National Instrument DAQ.

Then we record *VV* and *VH* components. *VV* represents the component corresponding to V-polarization incidence and V-polarization detection. *VH* represents the component with V-polarization incidence and H-polarization detection. Then we combine *VV* and *VH* to obtain the total intensity, *I*,

$$I = VV + VH \ , \quad (1)$$

And then we calculate DOP:

$$DOP = \frac{VV - VH}{VV + VH}, \quad (2)$$

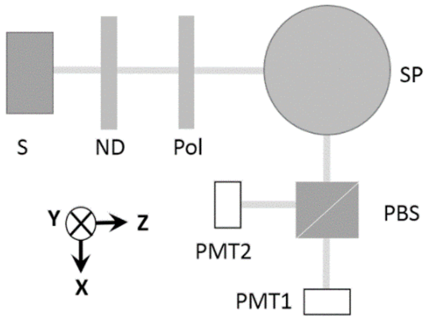

Fig.1, Schematic of the experimental setup. S: Light Source; ND: Neutral Density filter, Pol: Polarizer, SP: Sample, PBS: Polarizing Beam Splitter, PMT: Photomultiplier Tube.

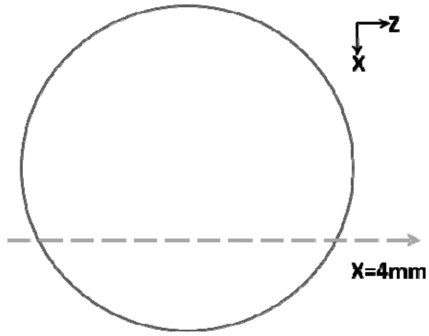

Fig.2, Scanning line across the fluid field, along Z direction and with x = 4mm.

As moving the sample at X and Z directions near the center area of the fluid, we measure the polarized-light scattering of the fibers in different field. In this paper, we scan the scattered light along Z axis, with x=4mm, which is shown as Fig.2.

III. Experimental Results

While scanning along Z axis with x = 4mm, we can record *VV* and *VH* and then obtain *I* and DOP. Fig. 3 shows how they vary along the different fluid field. From Fig.3 (a), one can find that along Z axis, *I* increases and reaches a peak and then drops to a trough, and finally increases slowly. And positions of the peak and trough have certain symmetry, that is z=-4mm and 4mm. Accordingly, from Fig.3 (b), DOP also varies and has the peak and trough at certain positions, even though these positions don't perfectly match with those of *I*. Additionally, there is a sub-peak around z=-8mm for DOP. Also, one can see that the dynamic range of *I* is less than 8 times, and that of DOP covers almost 0.2.

IV. Analysis and Discussion

A. Model

The experimental results can be explained by combining the principle of the scattering of the fibers with the stirred fluid field. We use the infinitely long solid cylinder to mimic the high- aspect-ratio glass fibers in the experiments. As shown in Fig.4, the scattering pattern of the infinitely long solid cylinder is a conical surface determined by the angle (η in Fig.4) between the incident light and the orientation of the cylinder [10]. The distribution of the scattering and the polarization of the angle (ξ in Fig.4) along the conical sectional circle is provided by the scattering theory of the cylinders [11].

In this paper, we set the incident direction of the light as Z axis. And the direction of the receiving arm determines the received scattering direction, which is in X-Z plane. According the geometry, one can find that, once these two directions are fixed, all the fibers whose scattering contributes to the signal, will fall in the angular bisection plane (ABP), which shown as Fig.5. This ABP bisects the angle between the incident direction and the scattering direction, and the intersecting line between ABP and X-Z plane is the angular bisection line (ABL in Fig.5). Particularly, in this paper, the scattering direction fall on X axis. So both ABP and ABL have 45° to Z axis.

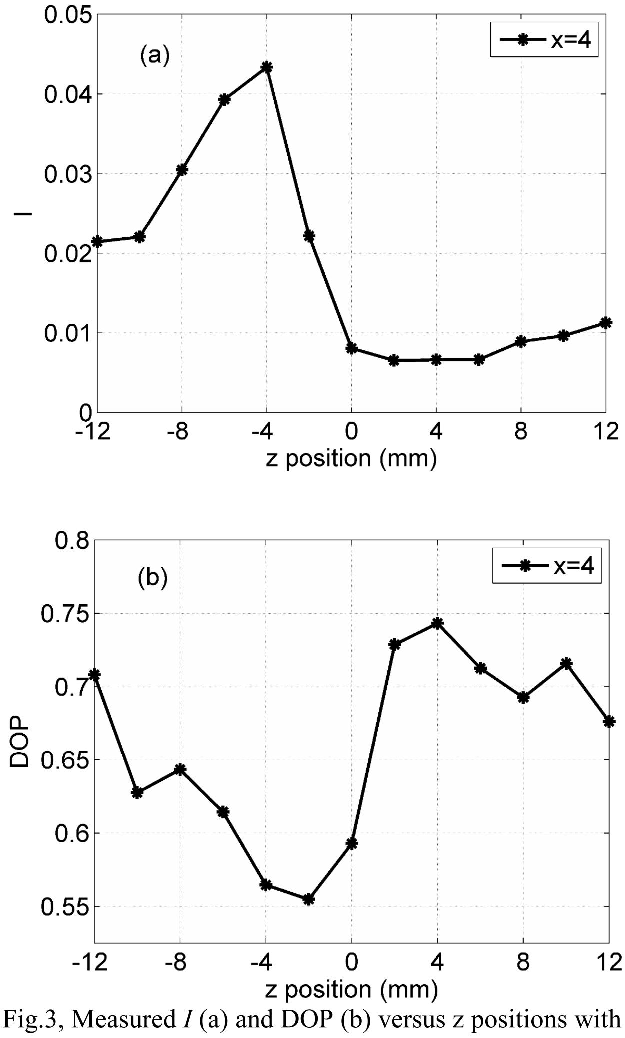

Fig.3, Measured *I* (a) and DOP (b) versus z positions with x = 4mm.

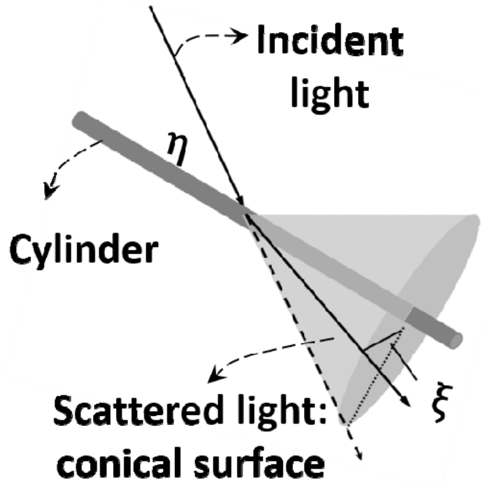

Fig.4, Sketch of the scattering of an infinitely long solid cylinder.

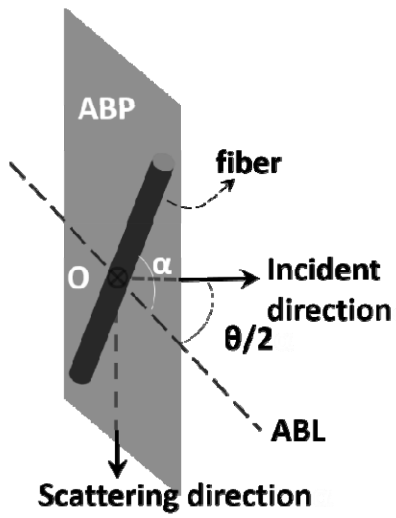

Fig.5, Description of the ABP and ABL, details shown in the text.

As being stirred, the fluid field near the center area is composed by the downwelling flow and concentric circular rotating flow, which is similar with the field generated by the impeller [12]. The movement of the cylindrical particles in the fluid field has complex structure and the relationship between the fluid and the particles are complicated [13-14]. Even so, for simplicity, in this paper, we assume that the orientation of the fibers in the scattering volume is same as the fluid field and could have a Gaussian distribution.

Based on these assumptions, we calculate the orientation of the fibers and the scattered intensity and DOP in the 90^o scattering direction. Then we can simulate the experiments, which is shown as Fig.6. From Fig.6 (a), one can find that the peak and trough appear at the similar position as the experimental results. And also, one can find the peak and trough in the DOP curve, shown as Fig.6 (b). And additionally, there is a sub-peak in DOP around z=-4mm, which responds similarly to the experimental result. So, the simulations can repeat qualitatively the results of the experiments. However, we also find that the dynamic range of *I* is almost 400 times and that of DOP is 0.4, both of which are larger than their counterpart of the experimental results.

B. Discussion.

According to the model, the fluid field are quite different along Z axis, which determines the orientations of the cylinders in each scattering volume vary with z positions. When scanning along Z axis, the received polarized-light scattering varies. For simplicity, the orientation of the cylinders in the scattering volume has certain Gaussian distribution, which has the main orientation determined by the model. When the main orientation of the cylinders at certain z position coincidently falls in ABP, the most of cylinders in the scattering volume contribute to the scattered intensity captured by the receiving arm, and then the maximal intensity reaches. However, if the main orientation of the cylinders is perpendicular to ABP, the least of cylinders contributes, and then minimal intensity reaches. As a result, we can find the peak and trough in both experiment and simulations.

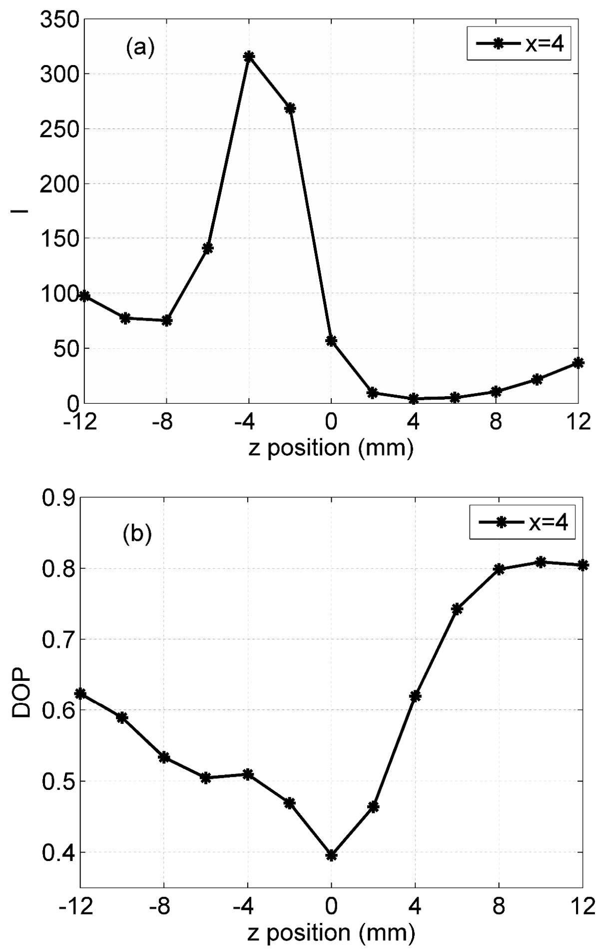

Fig.6, Simulated *I* (a) and DOP (b), based on the model.

For the received angle is 90°, ABL in the X-Z plane is 45° to Z axis. When the (x, z) = (4, -4), the orientation of the fluid field is 45° to Z axis, parallel with ABL, so the orientation of the fibers must fall in the ABP, and all scattering of them will contribute to the recorded signals. Then *I* reaches its maximum at this point. Inversely, for (x, z) = (4,4), the orientation of the field is 135 degree to Z axis, which is perpendicular to ABP. So in principle, all the fibers in the scattering volume would not contribute to the signal. But considering the distribution of the fibers, still a small number of them fall in ABP and then the intensity is not zero. The points located between these two points will have intermedia values. From the sharp drop of *I* around the peak, one can find that the ABP determined by the incident direction and the scattering direction plays a dominant role in the intensity of the signal.

For the related DOP, it also has peaks and troughs. But their position don't coincide with those of intensity. Both the main orientation and the distribution of the fibers have effects on the final polarization. We should keep in mind that for the setup, only the fibers oriented in ABP would contribute to the signals. So for different z positions, the fibers contributing to the signals only occupy certain part of ABP, which is determined by main orientation of the field and the width of Gaussian distribution. So, the polarization, different from the scale additivity of the intensity, should be considered in vector manner.

Since each scattering generates an intensity pulse, the signals consist of a time-series pulse. By analysis of these pulses and evaluating their DOP, we can give a preliminary statistics of scattered DOP for individual fiber. As shown in Fig.7, we can see that DOP dominates around 0.8, although the distribution can be clearly observed.

In the previous work, we calculate the full Stokes vector of the scattered light, and after normalizing it with the intensity, we obtained the three entries vector, namely S = [q, u, v]. We calculated a series of S with changing the orientation of the cylinders in the ABP. Then we found that in the space of S (3 dimensions), the orientation of cylinders can be solely determined by S [9]. Also, we plotted the results as a curve on the Poincare sphere. It is clear that the orientation of any fiber in the ABP corresponds to a unique point in the Poincare sphere, and vice versa, which means that we can determine the orientation of the fibers by measuring S of the scattered light [15].

Using simultaneous measurements of the Stokes vector and correlation analysis, we can also obtain the translation and rotational kinetics of the fibers suspended in stirred flow field [16]. In that paper, we found that the polarization is sensitive to the changes of the orientation of the fibers, and can be used to track it, and then characterize the movement of fibers in the scattering volume.

Additionally, the experimental data were obtained by replacing the receiving arm in Fig.1 (PBS, PMT1 and PMT2) with a GRIN lens Stokes polarimeter (GLP) [17] which is capable of measuring all the Stokes components within a single shot. The experimental results qualitatively agreed with the calculation. However, the current system still needs further improvement to increase its signal to noise ratio.

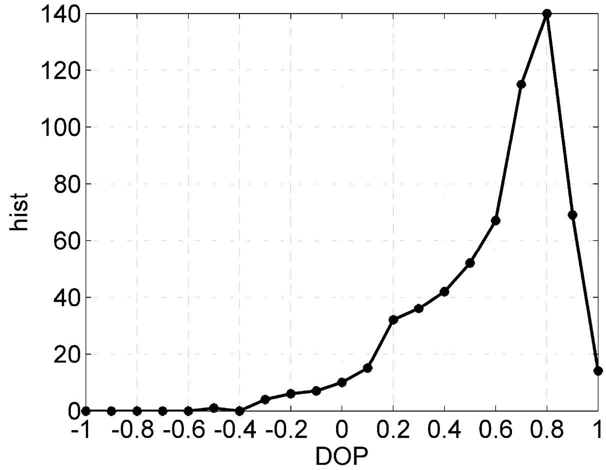

Fig.7, histogram of the DOP of individual fiber, and the measurement lasting for 10s.

V. CONCLUSION

Non-spherical particles dominate the particulates in the sea water. But current commercial detection tools always assume they are spherical shape. In this paper, we find that polarized-light scattering has the potential to retrieve the orientation of the suspended rod-shaped particles. A model based on the combination of the optical scattering of the cylinders and the fluid field, has been built to explain our experimental results of the suspended glass fibers, and the simulation can qualitatively repeat the results. The conclusion of the previous work says that the orientation of the fibers can be solely determined by the Stokes vector of the scattered polarization. And our new histogram of the DOP of the individual glass fiber, gives the hint that polarized-light scattering may be the potential method to detect the orientation of the suspended rod-shaped particles.

ACKNOWLEDGMENT

This work has been supported by National Natural Science Foundation of China (NSFC) (grant 41106034), China Postdoctoral Science Foundation (CPSF) (grant 20100480272), Shenzhen Innovation Foundation (grants JCYJ20140902110354247, JCYJ20140902110354241, JCYJ20140418095735582), and Joint Research Fund of Graduate Scholl at Shenzhen, Tsinghua University (grant JC2015001).

REFERENCES

[1] M. Twardowski, X. Zhang, S. Vagle, J. Sullivan, S. Freeman, H. Czerski, Y. You, L. Bi and G. Kattawar, "The optical volume scattering function in a surf zone inverted to derive sediment and bubble particle subpopulations," J. Geophys. Res. 117, C00H17, 2012.

[2] X. Zhang, M. Twardowski, and M. Lewis, "Retrieving composition and size of oceanic particle subpopulations from the volume scattering function," Appl. Opt. 50, 1240-1259, 2011.

[3] W. Clavano, E. Boss and L. Karp-Boss, "Inherent optical properties of non-spherical marine-like particles – from theory to observation," Oceanography and Marine Biology: An Annual Review, 45, 1-38, 2007.

[4] H. He, N. Zeng, R. Liao, T. Yun, W. Li, Y. He, and H. Ma, "Application of sphere-cylinder scattering model to skeletal muscle," Opt. Express 18, 15104-15112, 2010.

[5] R. Liao, N. Zeng, D. Li, T. Yun, Y. He, and H. Ma, "Penetration depth of linear polarization imaging for two-layer anisotropic samples," Appl. Opt.50, 4681-4687, 2011.

[6] R. Liao, N. Zeng, X. Y. Jiang, D. Z. Li, T. Yun, Y. H. He and H. Ma, "A rotating linear polarization imaging technique for anisotropic tissues," J. Biomed. Opt. 15, 030614, 2010.

[7] H. R. Gordon, "Light scattering and absorption by randomly-oriented cylinders: dependence on aspect ratio for refractive indices applicable for marine particles," Opt. Express 19, 4673-4691, 2011.

[8] B. Bronk, and S. D. Druger, "Light scattering calculations exploring sensitivity of depolarization ratio to shape changes. II. Single rod-shape vegetative bacteria in air," Appl. Opt. 48, 5655-5663, 2009.

[9] R. Liao and H. Ma, "Probing the suspended marine algae using polarized-light scattering," presented at Marine Technology Society (MTS)/Institute of Electrical and Electronic Engineers (IEEE) OCEANS Conference 2014, Taipei, 7–10 April 2014.

[10] T. Yun, N. Zeng, W. Li, D. Li, X. Jiang, and H. Ma, "Monte Carlo simulation of polarized photon scattering in anisotropic media," Opt. Express, 17, 16590–16602, 2009.

[11] C. F. Bohren and D. R. Huffman, Absorption and Scattering of Light by Small Particles, Wiley-Interscience, 1983.

[12] A. Brucato, M. Ciofalo, F. Grisafi and G. Micale, "Numerical prediction of flow fields in baffled stirred vessels: A comparsion of alternative modelling approachses", Chemical Engineering Science, 53(21), 3654-3684, 1998.

[13] M. Rahnama, D. L. Koch and E. S. G. Shaqfeh, "The effect of hydrodynamic interactions on the orientation distribution in a fiber suspension subject to simple shear flow," Phys. Fluids 7(3), 487-506, 1995.

[14] D. Zhang, D. Smith, D. A. Jack and S. Montgomery-Smith, "Numerical Evaluation of single fiber motion for short-fiber-reinforced composite materials processing," J. Manuf. Sci. Eng. 133, 051002, 2011.

[15] R. Liao, H. He, N. Zeng and H. Ma, "Characterizing the micro structure and kinetics of fast changing samples by simultaneous polarization measurements, " Proc. of SPIE 9322, 9322C-1, 2015.

[16] R. Liao, X. Ou and H. Ma, "Characterizing the kinetics of suspended cylindrical particles by polarizaiton measurements," presented in SPIE Optical Engineering + Applications, Polarization Science and Remote Sensing VII, 11-12 August, San Diego, 9613-39, 2015.

[17] J. Chang, N. Zeng, H. He, Y. He, and H. Ma, "Single-shot spatially modulated Stokes polarimeter based on a GRIN lens", 39(9), 2656-2659, 2014.